Published in final edited form as:
Mol Cancer Res. 2018 January ; 16(1): 3–15. doi:10.1158/1541-7786.MCR-17-0244.

PKCε Controls Mitotic Progression by Regulating Centrosome Migration and Mitotic Spindle Assembly

Silvia Martini[1,2], **Tanya Soliman**[2], **Giuliana Gobbi**[1], **Prisco Mirandola**[1], **Cecilia Carubbi**[1], **Elena Masselli**[1], **Giulia Pozzi**[1], **Peter J. Parker**[2,3], and **Marco Vitale**[1,4]

[1]Department of Medicine and Surgery, University of Parma, Parma, Italy (IT)

[2]Protein Phosphorylation Laboratory, Francis Crick Institute, London, United Kingdom (UK)

[3]King's College London, New Hunts House, Guy's Campus, London, United Kingdom (UK)

[4]CoreLab, Azienda Ospedaliero-Universitaria di Parma, Parma, Italy (IT)

Abstract

To form a proper mitotic spindle, centrosomes must be duplicated and driven poleward in a timely and controlled fashion. Improper timing of centrosome separation and errors in mitotic spindle assembly may lead to chromosome instability, a hallmark of cancer. Protein Kinase C epsilon (PKCε) has recently emerged as a regulator of several cell cycle processes associated with the resolution of mitotic catenation during the metaphase-anaphase transition and in regulating the abscission checkpoint. However, an engagement of PKCε in earlier (pre)mitotic events has not been addressed. Here, we now establish that PKCε controls prophase-to-metaphase progression by coordinating centrosome migration and mitotic spindle assembly in transformed cells. This control is exerted through cytoplasmic dynein function. Importantly, it is also demonstrated that the PKCε dependency of mitotic spindle organization is correlated with the non-functionality of the TOPO2A-dependent G2 checkpoint, a characteristic of many transformed cells. Thus, PKCε appears to become specifically engaged in a programme of controls that are required to support cells. Thus, PKCε appears to become specifically engaged in a programme of controls that are required to support cell cycle progression in transformed cells, advocating for PKCε as a potential cancer therapeutic target.

Implications—The close relationship between PKCε dependency for mitotic spindle organization and the non-functionality of the TOPO2A-dependent G2 checkpoint, a hallmark of transformed cells, strongly suggests PKCε as a therapeutic target in cancer.

Keywords

Mitosis; Mitotic spindle; Centrosome; PKCε; Dynein

Corresponding Author: Marco Vitale, M.D. Department of Medicine and Surgery, Unit of Anatomy and Histology, University of Parma, Ospedale Maggiore, Via Gramsci, 14. 43126 Parma, Italy, Ph.:+39.0521.033032, marco.vitale@unipr.it.

The authors declare no potential conflicts of interest.

Europe PMC Funders Author Manuscripts

Introduction

Bipolar spindle assembly is a highly coordinated process that requires the separation of the centrosome in prophase along the nuclear envelope and the interaction of microtubules emanating from the spindle poles with the kinetochores. This arrangement allows the duplicated chromosomes to be pulled to the opposite sides of the cell upon sister chromatid separation, thus leading to the formation of two daughter cells with an equal number of chromosomes. Improper timing of centrosome separation and errors in mitotic spindle assembly have been demonstrated to be a potentially frequent source of aneuploidy in human cancers (1–3).

Cytoplasmic dynein is a large motor protein involved in many cellular functions including microtubule organization, cell motility, intracellular trafficking and organelle positioning (4). Powering the movement along microtubules toward their minus ends, dynein plays critical roles in cell division, including early centrosome separation and bipolar spindle formation (5–7), cargo transport along microtubules (8–9), spindle positioning (10) and chromosome movement (11). Due to these multiple functions, dynein localizes to centrosomes, nuclear envelope (NE), mitotic spindle microtubules, kinetochores (KTs) and the cell cortex during G2 and mitosis (12–14).

Protein Kinase C epsilon (PKCε) is a serine/threonine kinase involved in tumor cell invasion and metastasis (15). PKCε is found frequently overexpressed in a wide variety of human cancers and has been implicated in malignant transformation of cells, including invasion and metastasis (16–19). Besides its oncogenic role, PKCε has been also implicated in proliferation and differentiation in different cell types (20–25). Furthermore, an emergent role for PKCε has been described in transformed cell models, in the resolution of mitotic catenation during the metaphase-anaphase transition and in regulating the completion of cytokinesis (26–30). Although it has been reported previously that the hypophosphorylated PKCε associates with CG-NAP in the centrosome area (31), a role in early (pre)mitotic events has not been established. Here we demonstrate that PKCε activity is required for proper centrosome migration in prophase, thus regulating prophase-to-metaphase progression. We identify cytoplasmic dynein as a PKCε binding partner and show that dynein inhibition phenocopies the inhibition of the kinase. In this novel scenario, by influencing dynein function, PKCε is positioned as a coordinator of prophase-to-metaphase progression. Importantly, we further demonstrate that PKCε has this role in mitotic spindle organization in transformed cell models, but not in “normal” diploid cells, consistent with the phenotype of the mouse knock-out and suggesting this emergent PKCε/dynein pathway as a potential therapeutic target.

Materials and Methods

Reagents

All reagents were obtained from Sigma Aldrich unless otherwise specified. ATM/ATR inhibitors, NaPP1, BIM-1, EHNA and Ciliobrevin were obtained from Calbiochem. Blu577 was obtained from Dr Jon Roffey, Cancer Research Technology, London, UK.

Cell lines

Cervix adenocarcinoma HeLa cells and colon adenocarcinoma DLD1-(GFP-PKCε-M486A) cells were routinely cultured in DMEM containing 10% fetal calf serum, antibiotics (50 U/mL penicillin, 50 μg/mL streptomycin) and were incubated at 37°C and 10% CO_2.

Erythroleukemia HEL 92.1.17 cells were routinely cultured in RPMI containing 10% FCS, antibiotics and incubated at 37°C and 5% CO_2.

Normal retina epithelial RPE1-hTERT were routinely cultured in DMEM containing 10% FCS, antibiotics and MEM Non Essential AminoAcids (Gibco), incubated at 37°C and 10% CO_2. HeLa, RPE-1, HEL 92.1.17 and DLD-1 cells were obtained from the cell services of the Francis Crick Institute, where are routinely screened for mycoplasma. Cells were passaged two or three times weekly at ratios between 1:5 and 1:10 and culture for the described experiments for 8/12 weeks between each collection.

Normal skin-derived immortalized human keratinocytes, clone NCTC 2544, were obtained from the American Tissue Culture Collection and cultured in EMEM medium (Euroclone, West York, UK) containing 10% fetal calf serum, L-glutamine (2 mM). Cells were passaged two or three times weekly at ratios between 1:5 and 1:10. Cell cultures were routinely assayed for mycoplasm contamination by Mycoalert mycoplasm detection kit (Lonza, Rockland, ME).

Normal Human Fibroblasts were kindly provided by Professor Bussolati, Department of Medicine and Surgery, University of Parma and established as previously 0 Cells were cultured in DMEM containing 20% FCS, antibiotics and incubated at 37°C and 5% CO_2. Cells were passaged at ratios between 1:2 and 1:5, kept in culture and used in the described experiments for 1 month after the collection. Cell cultures were assayed for mycoplasm contamination by Mycoalert mycoplasm detection kit (Lonza, Rockland, ME).

Cells synchronization and flow cytometry

HEL cells were synchronized in G_1/S border by culturing in growth medium supplemented with 2mM Thymidine for 16 h. Cells were washed and released into growth medium for 6 h and arrested in G_2/M border adding 10μM RO-3306 for 16 h. Cells were then released into growth medium for 90’ to obtain the population enriched in metaphase. To assess the efficiency of synchronization, aliquots of HEL cells blocked in G_1/S and G_2/M phases were permealized with 70% ethanol for 1h at 4°C, washed with PBS and incubated with PBS containing 20 μg/mL propidium iodide (PI) and 100 μg/mL RNAse-A for 15’ in dark room temperature before analysis. Analysis of samples was performed by FC500 flow cytometer (Beckman Coulter) and the Expo ADC software (Beckman Coulter).

DLD1-(GFP-PKCε-M486A) and HeLa cells were synchronized in metaphase by a sequential block and release with Thymidine and RO-3306. Cells were monitored using the Leica DM IL phase contrast microscope (40X/0.5NA) and cells were collected when 50-60% were in metaphase. DLD1-(GFP-PKCε-M486A) cell line was cultured with Doxycycline (100 ng/mL) overnight to induce expression of GFP-PKCε.

Formaldehyde crosslinking

Synchronized cells were scraped, pelleted and incubated using formaldehyde 1% at 4°C for 10min. Following a centrifugation 1800rpm for 3min, the cross-linking reaction was quenched with 1.25M Glycine/PBS, as described by Klockenbush C. and Kast J.(33).

Immunoprecipitation and immunoblotting

For co-immunoprecipitation experiments, HeLa cells were collected in ice cold RIPA buffer (50mM Tris pH 7.4, 150mM NaCl, 1mM EDTA, 1% Nonidet P-40, 0,1% SDS and 0.5% sodium deoxycolate) supplemented with fresh protease inhibitors and 1mM phenylmethylsulfonyl fluoride and incubated for 30min at 4°C. Lysed proteins were immunoprecipitated with Dynabeads Protein G (Invitrogen) for 1h at 4°C after coating with control IgM. Protein complexes were eluted with SDS 2X sample buffer after washing with RIPA buffer. Specifically, 10μg mouse anti-Dynein IC (Sigma Aldrich) and mouse-IgG (Santa Cruz) were used for immunoprecipitation. Proteins were resolved in 10% polyacrylamide gels and analyzed by immunoblotting using specific primary antibodies diluted as described by manufacturer's protocol. Specifically, rabbit anti-PKCε (Merck Millipore), mouse anti-Dynein IC (Sigma Aldrich).

For the endogenous protein expression analysis, the following antibodies were used: rabbit anti-PKCε (Merck Millipore), rabbit anti-PKCδ (Cell Signaling), rabbit anti-PKCβII (Santa Cruz), rabbit anti-PKCι (Abcam), rabbit anti-PKCθ (Abcam), mouse anti-glyceraldehyde-3-phosphate dehydrogenase (GAPDH) (Merck Millipore). Membranes were washed and incubated for 1 hour at room temperature with peroxidase-conjugated anti-rabbit (Thermo Scientific) or peroxidase-conjugated anti-mouse IgG (Thermo Fisher) and resolved by ECL Supersignal West Pico Chemiluminescent Substrate detection system (Thermo Fisher). Protein densitometric analysis was performed by using the ImageJ software system.

Pharmacological inhibition

DLD1-(GFP-PKCε-M486A) cell line was cultured with Doxocycline (100 ng/mL) 1μM NaPP1 to inhibit PKCε activity, as previously described(27). In HeLa, DLD1-(GFP-PKCε-M486A), HEL, RPE-1, NCTC2544, and human fibroblasts PKCε was inhibited using 1μM BIM-1 or 0.5μM Blu577, as previously described (29). Dynein activity was inhibited using 100μM EHNA or 20μM Ciliobrevin.

Co-IP using GFP-trap, proteolytic digestion and nanoLCMS analysis

All chemicals were purchased from Sigma at the highest grade possible unless otherwise stated. All solvents and nanoLC-MS additives were purchased as LC-MS grade from Fisher Scientific. DLD1-(GFP-PKCε-M486A) cells synchronized in G1/S, G2/M and metaphase were scraped, pelleted and incubated for cross-linking reaction as described above. All samples were Co-Immunoprecipitated using GFP-Trap (Chromotek). Proteins were separated using a SDS-PAGE gel (NuPAGE 3-8% Tris-Acetate gel (Invitrogen) for short gel lane extraction for MS analysis and 8 bands from each lane were excised and processed further using the previously described in gel digestion procedure adapted for a Janus liquid handling system (Perkin Elmer). 10 μL of gel extracted peptides in 1 % acetonitrile and 1 % formic acid in water were analysed by nano liquid chromatography in tandem with mass

spectrometry (nanoLCMS) using an Acquity UPLC (Waters) connected to a LTQ Orbitrap XL Mass Spectrometer (Thermo Scientific). Raw files containing MS spectra were processed using a protein database search, carried out using MaxQuant (version 1.5.2.8) as previously described, against a UniProt human database. Intensity-based absolute quantification (iBAQ) was utilised for label free quantitation of the reported proteins. Data was then further analysed using Perseus (version 1.4.0.2).

Live-cell imaging

For videomiscroscopy experiments, cells were cultured on LabTek chambered coverglass slides (Nunc) in Liebovitz CO_2-independent media (Gibco). All experiments were performed at low light level inverted microscope (Nikon TE2000) imaging system equipped with a lamina-flow heater maintaining a constant temperature of 37±0.01°C, a Plan-Fluor 40X DIC lens and a Xenon lamp for fluorescence excitation. Images were taken using a high quantum efficiency charge coupled device camera (Andor Ixon) every 3 minutes.

Immunofluorescence microscopy and image analysis

Adherent cells were grown on 13mm glass coverslips and fixed and permeabilized with PHEM buffer (60mM PIPES pH6.8, 25mM HEPES pH7.4, 10mM EGTA pH8, 4mM $MgSO_4$, 4% paraformaldeyhyde and 0.1% Triton X-100) for 20min. HEL samples were fixed in methanol for 5’ at -20°C, centrifuged onto 1 μg/mL poly-*l*-lysine-coated 10mm coverslips, permeabilized with 0,5% Triton X-100 for 7min. Cells were then blocked using 3% BSA/PBS and probed using the following primary antibodies in 3% BSA/PBS: mouse anti-Dynein IC (Sigma Aldrich), mouse anti-p150(Glued) (BD Transduction Laboratory), mouse anti-BubR1 (Novus Biologicals), rabbit anti-phosphoCENP-A (S7) (Cell Signaling Technology), human anti-centromere (ACA) (Antibodies Inc.15-234-0001), mouse anti-αtubulin (Sigma Aldrich), rabbit anti-αtubulin (AbCam), rabbit anti-PKCε (Abcam). The secondary antibodies used were obtained from Thermo Fisher Scientific and were all used diluted in 3% BSA/PBS: goat anti-rabbit and goat anti-mouse Alexa Fluor 549, goat anti-rabbit e goat anti-mouse Alexa Fluor 488 and goat anti-human Alexa Fluor 647 (Thermo Fischer). All coverslips were mounted using ProLong Gold with DAPI (Invitrogen).

HeLa images were acquired using Carl Zeiss LSM 780 confocal microscope equipped with a X63 Plan-APOCHROMAT DIC oil-immersion objective and serial 1μM Z-sections were taken. Image analysis was carried out using Metamorph image analysis software. HEL, DLD1-(GFP-PKCε-M486A), NCTC2544 and human fibroblasts were examined with a Nikon Eclipse 80i (Tokyo, Japan) fluorescent microscope equipped with Nikon Plan color 40X/0.75 and Nikon Plan Apo VC 100X/1.4 oil immersion objective. Images were obtained using Nikon Camera DS-JMC and images acquisition was performed using Nis element F2.30 (Nikon, Japan). Image analysis was performed using ImageJ software.

In situ Proximity Ligation Assay (PLA)

The DuoLink *in situ* PLA kit (Olink Bioscience) with the DuoLink *in situ* Detection Reagent Orange (Sigma Aldrich) was used to detect PKCε/Dynein interaction according to the manufacturer’s protocols. HeLa cells were grown on 8-well CultureSlides (Falcon) overnight and treated with or without Blu557 for 1h. Cells were subsequently fixed and

permeabilized with PHEM buffer and blocked with 3% BSA/PBS. The slides were directly used for the assay and primary antibody mix solution containing anti-PKCε (AbCam) and anti-DyneinIC (Sigma Aldrich) diluted in 3% BSA/PBS was added to each sample and incubated in a humidity chamber for 1h at room temperature. Mouse IgG and Rabbit IgG (Santa Cruz) were used as negative controls. The assay was subsequently performed following the manufacturer instructions. The slides were mounted with ProLong Gold with DAPI (Invitrogen). Images were acquired using Carl Zeiss LSM 780 confocal microscope equipped with X63 Plan-APOCHROMAT DIC oil-immersion objective and analyzed and serial 1μm Z-sections were taken using ZEN image analysis software. Z-sections were summed and PKCε/Dynein interaction was quantified counting the number of signals each field counted using Image J.

PKCε down-regulation

For short hairpin RNA (shRNA)-based gene silencing, HEL cells were infected and were subsequently cultured in the presence of puromycin (2μg/mL), to select infected, puromycin-resistant cells. Cells were then collected after 5 days of puromycin-selection. The pLKO.1 lentiviral vector encoding shRNA against human PKCε (NM_005400; shPKCε) were obtained from Open-Biosystem (Thermo Fisher Scientific). As control (shRNA CT), we used the MISSION pLKO.1-puro Non-target shRNA Control Plasmid, not targeting any known genes (Sigma-Aldrich). The shRNA expressing viruses were produced in 293TL cells according to standard protocols. For siRNA transfection, HiPerfect (Quiagen) was used according to the manufacturer's recommendations; all siRNAs were used at the final concentration of 10nM. siScramble1 and siPKCε1: PKCε expression levels were down-regulated by transfection of double-stranded siRNAs (dsRNA) designed to target sequences corresponding to nt 223 to 244, 429 to 450, 942 to 963, and 1158 to 1179 on human PKCεmRNA(NM005400). The target sequences are the following: 5′-AAGATCAAAATCTGCGAGGCC-3′, 5′-AAGAT CGAGC TGGCTG TCTTT-3′, 5′-AACTA CAAGG TCCCT ACCTTC-3′, and 5′-AAAAAGCTCATTGCTGGTGCC-3′. The respective sense and antisense RNA sequences were synthesized by the Silencer siRNA Construction Kit (Ambion). siScramble 2 was purchased from Quiagen: cat. 1027310 (5'-AATTCTCCGAACGTGTCACGT-3'). siPKCε2 was purchased as SmartPool from Dharmacon: siGenome PKCε siRNA Cat.D-004653(5'-GGGCAAAGAUGAAGUAUAU-3') and Cat.J-004653-08-0050(5'-GACGUGGACUGCACAAUGA-3').

Statistical tests

Statistical analyses were performed by using one-way analysis of variance or *t*-test when applicable. Prism software (Graphpad) was used for all the calculations. The level of statistical significance is represented as follows: n.s.=P>0.05, *=P<0.05,**=P<0.01, ***=P<0.001, ****P<0.0001.

Results

PKCε inhibition affects mitotic spindle morphology

A role for PKCε in mitosis has been established previously (26–30). However, a cell cycle function preceding onset of mitosis is not documented. We used immunofluorescence microscopy to investigate PKCε subcellular localization in the early stages of mitosis. PKCε localizes to the centrosomes from G2/M phase to metaphase, in a pattern identical to that of γ-tubulin (Fig.1a). To assess the effects of PKCε inhibition, HeLa cells were treated for 1 hour with Bisindolylmaleimide 1 (BIM-1), a protein kinase C inhibitor, or Blu577, a structurally unrelated and more selective PKCε inhibitor. PKCε localization at the centrosome is not affected by the treatment with either inhibitor (Fig.1b). In contrast to control cells, in which the microtubules were organized into well-defined radial arrays, Blu577- and BIM-1-treated cells showed an unfocused and disoriented mitotic spindle with misaligned chromosomes (Fig.1c). Strikingly, PKCε inhibition by Blu577 results in a significant higher percentage of cells (52±4%) which display abnormal mitotic spindle morphology compared to the control (15.66±2.88% ($P<0.001$ *vs* CT)) (Fig.1d). BIM-1 treatment results in a stronger effect on mitotic spindle organization than Blu577 (72±4.36% ($P<0.01$ *vs* Blu577)). This might be due to the broader effect of BIM-1, which is able to inhibit not only PKCε but other PKC isoforms including PKCβ, which have previously been implicated in microtubule organization and spindle function (34). To confirm this finding, we treated HeLa cells with two different small interfering RNAs (siRNA) to down-regulate PKCε expression for 48 hours (Fig.1e,f). Note that no effect of PKCε knockdown on other PKC isoforms was found (Fig.S1a,b). Consistently, following PKCε knockdown, we observed an increase in the number of cells in metaphase with defects in mitotic spindle structure in siPKCε-transfected cells, compared with siScramble controls. Several others PKC isoforms have been reported to be centrosome-associated (34–37). However, using siRNA, chemical biology and drugs we here demonstrate the involvement of PKCε in mitotic spindle organization.

Inhibition of PKCε results in a delayed metaphase entry due to prolonged centrosome migration

We imaged unsynchronized HeLa cells stably expressing mCherry-H2B and GFP-Tubulin by time-lapse video-microscopy and recorded the time taken from prophase, when the centrosomes are duplicated and the DNA is condensed, to metaphase alignment (Fig.2a; Fig.S1c). Most control cells (58%) took from 3 to 9 minutes to reach metaphase alignment. This frequency is dramatically reduced upon treatment with Blu577 or BIM-1 (2.2±2% Blu577, 2.5±1% BIM-1) (Fig.2b). As shown in Figure 2a, a representative control cell reaches metaphase alignment in 9 minutes from prophase, whereas the cell treated with Blu577 is still in prophase/prometaphase at this time point. Consistently, PKCε inhibition causes a delay in metaphase entry, as illustrated in the cumulative frequency graphs in Figures 2b and S2a, showing an increase in the number of cells taking from 10 to 20 minutes (42±7.6% Control *vs* 57.4 ± 3% Blu577 and 58.3%±0.5 BIM-1) or between 21 and 39 minutes to transit from prophase to metaphase (3±0.4% Control *vs* 40.4±1.3% Blu577 and 39.3±1.7% BIM-1). In line with the delay to metaphase entry, we also observed a lag in the timing of centrosome movement toward the opposite poles. We scored the time that

centrosomes took from their duplication, until they are positioned to the opposite poles assembling the bipolar spindle. Duplicated centrosomes of untreated HeLa cells did not take more than 6 minutes to migrate, whereas upon Blu577 and BIM-1) treatment, centrosomes took more than 10 minutes (17±5% ($P<0.001$)) and 30.5±6.5% ($P<0.001$ *vs* Control) minutes, respectively) (Fig.2c). In addition, we observed in cells treated with PKCε inhibitors an aberrant morphology of the spindle that we refer to as “bending” phenotype (white arrow, Fig.2a;Fig.2c), which correlates with the delay in centrosome movement and consequent mitotic spindle disorganization observed by confocal imaging (Fig.2a and 2d). In accordance with the critical role of PKCε in cytokinesis (26) the number of cells unable to complete cytokinesis is increased upon PKCε inhibition (Fig.S1d).

Identification of Cytoplasmic Dynein and PKCε as binding partners in G2/M

We used tandem mass spectrometry fingerprinting in order to identify potential PKCε binding partners throughout mitosis. Among the known spindle-associated proteins reported, Dynein Heavy Chain 1 was found to bind PKCε in G2/M and metaphase (Fig.3a). We confirmed the PKCε interaction with Dynein by co-immunoprecipitation of the endogenous proteins in HeLa cells. PKCε physically interacts with Dynein in cells synchronized in metaphase (Fig.3b). To confirm and determine the subcellular localization of PKCε/Dynein interaction, we used an *in situ* proximity ligation assay (PLA). This assay revealed that PKCε interacts with Dynein around the nuclear envelope and chromatin in prophase, and in the mitotic spindle region in prometaphase and metaphase (Fig.3c). No PLA signal was detected in the negative control (Fig.3d). Our findings suggested an involvement of PKCε in mitotic spindle organization and mitotic progression. Since Dynein plays critical roles in centrosome separation and bipolar spindle assembly, we hypothesised that PKCε supports Dynein function and regulates prophase-metaphase progression in these cells.

Dynein ATPase activity inhibition phenocopies inhibition of PKCε

To investigate whether PKCε regulates Dynein function, we treated HeLa cells with EHNA (Erythro-9-3-(2-hydroxynonyl)adenine), to inhibit Dynein ATPase activity and interfere with Dynein binding with microtubules (38). One hour inhibition of Dynein activity caused aberrations in mitotic spindle morphology comparable with the spindle defect seen when HeLa cells were treated with Blu577 and BIM-1 (Fig.4a). Cells treated with EHNA showed a defective mitotic spindle when compared with control (84±6%;$P<0.001$) (Fig.4b). HeLa cells were then imaged by time-lapse microscopy following treatment with EHNA (Fig.4d). As expected, Dynein inhibition resulted in a delay of centrosome movement, thereby delaying mitotic progression. Indeed, prophase to metaphase alignment transition is delayed in most EHNA-treated cells: 61±4 % of cells took from 10 to 20 minutes to transit and 33±5% of cells took from 21 to 39 minutes to reach metaphase alignment (Fig.4c and FigS2b). Interestingly, the very slow transiting cells (21-39 min) were unable to properly complete mitosis, indicating that the multiple functions exerted by Dynein throughout mitosis are essential for the proper completion of cell division. Further, we noted the “bending” behaviour of GFP-Tubulin, which was very similar to the phenotype seen with PKCε inhibition (Fig.4e,f). The same bending behavior was also observed in cells treated with a different dynein inhibitor, Ciliobrevin (39)(Fig.S2). Collectively, these data indicate

that inhibition of Dynein phenocopies PKCε inhibition and indicates that PKCε acts with Dynein in the prophase to metaphase transition.

Dynein accumulates at kinetochores upon PKCε inhibition

Immunofluorescence microscopy studies demonstrated that dynein localizes to kinetochores prior to MTs attachment, where it regulates initial interactions with spindle fibres and coordinates the early aspects of chromosome movement in prometaphase (40,41). As chromosomes achieve bipolar attachment, kinetochore dynein staining becomes less prominent and is undetectable once the chromosomes are aligned. Loss of dynein at the kinetochores coincides with an enhanced labelling along the spindle fibres and spindle poles. Since PKCε inhibition results in a prolonged prometaphase, we investigated dynein localization using immunofluorescence in HeLa cells treated for 1hour with Blu577 or BIM-1. Untreated HeLa cells in metaphase displayed Dynein labelling on the spindle fibres and at the spindle poles, at the plus end of MTs and at the cortex at one side of the cell (Fig. 5a). By contrast, HeLa cells treated with PKCε inhibitors showed a disorganised spindle morphology with chromosomes in a prometaphase-like state and an enrichment of Dynein at the kinetochores and at the plus end of unattached MTs. Indeed, double staining of Dynein and the chromatin-associated protein phospho-CENP-A (Ser7) upon PKCε inhibition confirmed the Dynein localization at the kinetochores (Fig.5b). In an unsynchronized population of HeLa cells, Dynein localization at the kinetochores is detectable in the 2±1% of cells compared with 37±4 % and the 50±2 % of cells treated with Blu577 and BIM-1 respectively ($P<0.001$) (Fig.5c). This is in line with our previous observation that inhibition of PKCε in an unsynchronized population of cells results in a delay of metaphase entry, sustaining the notion that PKCε is required for prophase to metaphase progression. In addition, Dynein localization at the kinetochores can be explained as a perturbation of Dynein streaming from the plus ends of microtubules to the spindle poles, in line with the hypothesis that Dynein activity is regulated by PKCε. We therefore examined Dynein localization in cells treated with EHNA. As expected, EHNA treatment resulted in a higher percentage of cells with a disorganized mitotic spindle and Dynein enrichment at the kinetochores. This phenotype is similar to that seen upon Blu577 and BIM-1 treatment, concordant with our observation that Dynein inhibition phenocopies PKCε inhibition (Fig. 5c,Fig.S3a). EHNA treatment revealed also a new localization of PKCε at the kinetochores, as confirmed by the double staining with the centromere antibody CREST (Fig.S3b,c).mWe showed that Dynein interacts with PKCε in prometaphase and the inhibition of Dynein and PKCε result in an accumulation of both proteins at the kinetochores. This suggests that in prometaphase, the PKCε/Dynein complex is trapped at the kinetochores when either of the proteins are inhibited. We also examined the localization of p150 (Glued), the largest subunit of Dynactin complex, which links Dynein to cargos and increases its processivity (42). As for Dynein, but with a less profound effect, Dynactin localized at the kinetochores to a significantly higher extent in cells treated with PKCε inhibitors indicating that not only Dynein, but the Dynein/Dynactin complex becomes more stably localized at the kinetochores when PKCε is inhibited (Fig.S3d,e).

A prediction arising from the delayed movement and organization of productive kinetochore-microtubule (K-MT) engagement, is that in unsynchronized cells, there will be

an increase in the steady state presence of APC/C regulators such as BubR1(43) at the kinetochore (BubR1 poleward streaming is K-MT and dynein-dependent and is abolished upon dynein inhibition (44,45)). We assessed therefore whether PKCε inhibition influences BubR1 retention at kinetochores following treatment with Blu577 or BIM-1 (Fig.S3f). PKCε inhibition resulted in a higher percentage of cells with a kinetochore accumulation of BubR1 compared to controls, consistent with the delay in productive K-MT formation(Fig. 5d,e). This is comparable with EHNA treatment which, as expected, caused an increase in the number of cells retaining both BubR1 and PKCε at the kinetochores. Note that this delayed K-MT organization is distinct from the delayed release of BubR1 associated with a catenation triggered metaphase/anaphase transition (the latter is associated with the loss of Mad2 from kinetochores while the delay observed here is associated with retention of kinetochore Mad2; data not shown).

PKCε regulates mitotic spindle assembly in transformed cell models

It has been demonstrated previously that PKCε is a regulator of the metaphase catenation response, following escape from the G2 Topoisomerase-2 dependent checkpoint (27). Defects in the G2 checkpoint are a characteristic of many transformed cells (28,46). Here we showed that PKCε inhibition results in defects in mitotic spindle organization with consequent delay in mitotic progression in HeLa cells. Therefore, we sought to determine whether the abnormal mitotic spindle morphology caused by PKCε inhibition was restricted to transformed cell models. As observed in HeLa cells, PKCε localized at the centrosomes in the additional transformed cell lines HEL and DLD-1(PKCεM486A) (Fig.S4a,b). The PKCε dependency for mitotic spindle assembly was assessed by treating HEL and DLD-1(PKCεM486A) for 1 hour with Blu577 (Fig.6a). Similarly to what was observed in HeLa cells, the number of cells in metaphase with defective mitotic spindles is significantly higher in HEL (43.10±0.34%) and DLD-1 cells (52 % ± 5.29) treated with Blu577, compared with controls (9.44% ± 0.79 HEL and 16 % ± 2.65 DLD1;$p<0.001$). To confirm this finding, we used specific shRNA and siRNA to downregulate the expression of PKCε in HEL cells and the ATP analog NaPP1 to inhibit the gate-keeper modified kinase in the DLD-1 cell line(27,47). Consistently, in both cell lines we observed an increase in the number of mitotic cells with abnormal spindle geometry upon PKCε inhibition, confirming that PKCε is necessary for mitotic spindle assembly (Fig.6b-d;Fig.S4f). We further assessed PKCε localization in “normal” diploid cell lines: normal human keratinocytes (NCTC 2544), primary human fibroblasts and non-transformed RPE1-hTERT cells showed PKCε enrichment at the centrosomes as the transformed cell lines (Fig.S4g). therefore, we investigated PKCε inhibition response in non-transformed cell lines by treating cells with Blu577 under the same conditions as the transformed cells. Although PKCε inhibition resulted in a higher number of cells with spindle defects, compared to control cells (Fig.S4h), this percentage is significantly lower compared with transformed cell lines (Fig. 6e); only 6.2 ± 0.68% RPE1-hTERT cells, respond to PKCε inhibition with an abnormal spindle morphology. These results suggest that the PKCε dependency of mitotic spindle organization is related to the transformed status of cells.

Discussion

We have investigated the effects of PKCε inhibition in early mitotic events by using different methods of inhibition in multiple transformed cell models (HeLa human cervical carcinoma, HEL human erythroleukemia and DLD1 human colorectal adenocarcinoma). Consistently, cells in prometaphase from all cell lines displayed an abnormal mitotic spindle morphology compared with controls, implicating the involvement of PKCε in bipolar spindle assembly. Interestingly, this was not the case in the 'normal' keratinocytes NCTC2544, primary human fibroblasts and the non-transformed retinal pigment epithelium RPE1-hTERT cell lines. The G2/M catenation checkpoint is defective in several cell lines, including HeLa cells, whereas it is functional in 'normal' cells (46). Brownlow et al. have previously demonstrated that cells with a leaky G2 catenation checkpoint are dependent on PKCε for catenation resolution in mitosis (28). In an interesting alignment with this finding, we suggest that the dependence on PKCε for mitotic spindle assembly is related to the transformation status of the cell. These finding suggests that PKCε inhibition leads to a delay of metaphase transit in transformed cells, increasing the risk of failure in MTs/kinetochores attachment and potentially contributing to genomic instability.

Live-cell imaging of asynchronous HeLa cells revealed that PKCε inhibition causes a delay of centrosome migration to the opposite sides of the nucleus. Nevertheless, increasing microtubule nucleation at centrosomes occurs and a mitotic spindle is assembled albeit showing an abnormal morphology, a 'bending' phenotype. This might reflect the dominance of chromosome arm engagement and the kinesin-10 dependent chromosome organization i.e. the polar ejection force (48). The centrosome movement delay and the 'bending' phenotype caused by PKCε inhibition are likely to interfere with the kinetochore capture by the mitotic microtubules, leading to a delay to metaphase entry.

Among the several motor proteins implicated in cell division, cytoplasmic dynein is a microtubule motor complex, which plays key roles in multiple processes, such as centrosome separation and spindle organization. How cytoplasmic dynein is able to fulfill such a wide range of processes in cell division is still unclear, making it challenging to address functions attributed to specific dynein pools. However, it has been demonstrated that the interaction with multiple adaptor proteins is essential to orchestrate the timing and localization of dynein functions (49). Here we demonstrate that PKCε physically and functionally interacts with cytoplasmic dynein from G2/M phase to metaphase. Indeed, the phenotypes observed upon dynein inhibition are comparable with the effects of PKCε inhibition, suggesting that PKCε and dynein are functionally related.

After nuclear envelope breakdown, dynein is recruited to the kinetochores where it regulates proper microtubule attachment and chromosome alignment in prometaphase. Defects in kinetochore-microtubule (KC-MT) attachment and the spindle assembly checkpoint (SAC) during cell division are strongly associated with genomic instability. The SAC is active during prometaphase and once the chromosomes are aligned and the mitotic spindle is correctly assembled in metaphase, dynein moves from the kinetochores along the microtubules streaming the proteins involved in the SAC, such as BubR1.

Europe PMC Funders Author Manuscripts

It has been shown that PKCε plays a role partially antagonistic with dynein streaming in G2 checkpoint compromised cells, where delayed metaphase progression is triggered by sister chromatid catenation consequent to treatment with ICRF-193(28). Here cells are delayed in progressing to anaphase by PKCε action, characterised by the retention of BubR1 at the kinetochores and a non-silenced SAC. We show evidence here that PKCε inhibition causes the accumulation of both dynein and BubR1 at the kinetochores in asynchronous HeLa cells, indicating that PKCε inhibition compromises kinetochore-microtubule attachment thereby influencing the dynein-dependent streaming and delaying sister chromatids alignment in metaphase. The interaction of PKCε and dynein (as determined by co-immunoprecipitation and PLA) suggests that PKCε may act as a general regulator of dynein function modifying cargo selection perhaps both in prometaphase (as described here) and at anaphase entry (28).

Taken together, the presented data demonstrate that PKCε modulates prophase-to-metaphase progression in transformed cell models, by regulating centrosome migration and mitotic spindle organization via dynein interaction. These findings and those reported previously (26–30) establish PKCε as a key regulator of cell cycle progression where there are DNA-associated stresses encountered. In conclusion, the close relationship between PKCε dependency for mitotic spindle organization and the non-functionality of G2 checkpoint(s), (a hallmark of transformed cells), is a strong prescription for PKCε as a therapeutic target in cancer.

Supplementary Material

Refer to Web version on PubMed Central for supplementary material.

Acknowledgements

We thank Luciana Cerasuolo, Vincenzo Palermo, Domenico Manfredi and Davide Dallatana, University of Parma, Italy, for technical support. We also thank the Francis Crick Institute (LRI) facilities for the valuable support, in particular the Light Microscopy and the Protein Analysis and Proteomics technology platforms, Francis Crick Institute, London, UK.

Financial support: This work was supported by Regione Emilia-Romagna Area 1 – Strategic Program 2010-2012 to G. Gobbi.

References

1. Silkworth WT, Nardi IK, Paul R, Mogilner A, Cimini D. Timing of centrosome separation is important for accurate chromosome segregation. Mol Biol Cell. 2012; 23(3):401–11. [PubMed: 22130796]
2. Fukasawa K. Oncogenes and tumour suppressors take on centrosomes. Nat Rev Cancer. 2007; 7(12): 911–24. [PubMed: 18004399]
3. Nam HJ, van Deursen JM. Cyclin B2 and p53 control proper timing of centrosome separation. Nat Cell Biol. 2014; 16(6):538–49. [PubMed: 24776885]
4. Roberts AJ, Kon T, Knight PJ, Sutoh K, Burgess SA. Functions and mechanics of dynein motor proteins. Nat Rev Mol Cell Biol. 2013; 14(11):713–26. [PubMed: 24064538]
5. Vaisberg EA, Koonce MP, McIntosh JR. Cytoplasmic dynein plays a role in mammalian mitotic spindle formation. J Cell Biol. 1993; 123(4):849–58. [PubMed: 8227145]
6. Tanenbaum ME, Macůrek L, Galjart N, Medema RH. Dynein, Lis1 and CLIP-170 counteract Eg5-dependent centrosome separation during bipolar spindle assembly. EMBO J. 2008; 27(24):3235–45. [PubMed: 19020519]

7. Raaijmakers JA, van Heesbeen RG, Meaders JL, Geers EF, Fernandez-Garcia B, Medema RH, et al. Nuclear envelope-associated dynein drives prophase centrosome separation and enables Eg5-independent bipolar spindle formation. EMBO J. 2012; 31(21):4179–90. [PubMed: 23034402]
8. Young A, Dictenberg JB, Purohit A, Tuft R, Doxsey SJ. Cytoplasmic dynein-mediated assembly of pericentrin and gamma tubulin onto centrosomes. Mol Biol Cell. 2000; 11(6):2047–56. [PubMed: 10848628]
9. Silva PM, Reis RM, Bolanos-Garcia VM, Florindo C, Tavares ÁA, Bousbaa H. Dynein-dependent transport of spindle assembly checkpoint proteins off kinetochores toward spindle poles. FEBS Lett. 2014; 588(17):3265–73. [PubMed: 25064841]
10. Kiyomitsu T, Cheeseman IM. Chromosome- and spindle-pole-derived signal generate an intrinsic code for spindle position and orientation. Nat Cell Biol. 2012; 14(3):311–7. [PubMed: 22327364]
11. Collins ES, Balchand SK, Faraci JL, Wadsworth P, Lee WL. Cell cycle-regulated cortical dynein/dynactin promotes symmetric cell division by differential pole motion in anaphase. Mol Biol Cell. 2012; 23(17):3380–90. [PubMed: 22809624]
12. Whyte J, Bader JR, Tauhata SB, Raycroft M, Hornick J, Pfister KK, et al. Phosphorylation regulates targeting of cytoplasmic dynein to kinetochores during mitosis. J Cell Biol. 2008; 183(5):819–34. [PubMed: 19029334]
13. Dujardin DL, Vallee RB. Dynein at the cortex. Curr Opin Cell Biol. 2002; 14(1):44–9. [PubMed: 11792543]
14. Tanenbaum ME, Akhmanova A, Medema RH. Dynein at the nuclear envelope. EMBO Rep. 2010; 11(9):649. [PubMed: 20805838]
15. Gorin MA, Pan Q. Protein kinase C epsilon: an oncogene and emerging tumor biomarker. Mol Cancer. 2009; 8:9.doi: 10.1186/1476-4598-8-9 [PubMed: 19228372]
16. Basu A, Sivaprasad U. Protein kinase Cepsilon makes the life and death decision. Cell Signal. 2007; 19(8):1633–42. [PubMed: 17537614]
17. Gobbi G, Masselli E, Micheloni C, Nouvenne A, Russo D, Santi P, et al. Hypoxia-induced down-modulation of PKCepsilon promotes trail-mediated apoptosis of tumor cells. Int J Oncol. 2010; 37(3):719–29. [PubMed: 20664941]
18. Gutierrez-Uzquiza A, Lopez-Haber C, Jernigan DL, Fatatis A, Kazanietz MG. PKCε Is an Essential Mediator of Prostate Cancer Bone Metastasis. Mol Cancer Res. 2015; 13(9):1336–46. [PubMed: 26023164]
19. Garg R, Benedetti LG, Abera MB, Wang H, Abba M, Kazanietz MG. Protein kinase C and cancer: what we know and what we do not. Oncogene. 2014; 33(45):5225–37. [PubMed: 24336328]
20. Queirolo V, Galli D, Masselli E, Borzì RM, Martini S, Vitale F, et al. PKCε is a regulator of hypertrophic differentiation of chondrocytes in osteoarthritis. Osteoarthritis Cartilage. 2016; 24(8):1451–60. [PubMed: 27072078]
21. Galli D, Carubbi C, Masselli E, Corradi D, Dei Cas A, Nouvenne A, et al. PKCε is a negative regulator of PVAT-derived vessel formation. Exp Cell Res. 2015; 330(2):277–86. [PubMed: 25433270]
22. Gobbi G, Mirandola P, Carubbi C, Galli D, Vitale M. Protein kinase C ε in hematopoiesis: conductor or selector? Semin Thromb Hemost. 2013; 39(1):59–65. [PubMed: 23266964]
23. Di Marcantonio D, Galli D, Carubbi C, Gobbi G, Queirolo V, Martini S, et al. PKCε as a novel promoter of skeletal muscle differentiation and regeneration. Exp Cell Res. 2015; 339(1):10–9. [PubMed: 26431586]
24. Carubbi C, Masselli E, Martini S, Galli D, Aversa F, Mirandola P, et al. Human thrombopoiesis depends on Protein kinase Cδ/protein kinase Cε functional couple. Haematologica. 2016; 101(7):812–20. [PubMed: 27081176]
25. Masselli E, Carubbi C, Gobbi G, Mirandola P, Galli D, Martini S, et al. Protein kinase Cε inhibition restores megakaryocytic differentiation of hematopoietic progenitors from primary myelofibrosis patients. Leukemia. 2015; 29(1):2192–201. [PubMed: 26183534]
26. Saurin AT, Durgan J, Cameron AJ, Faisal A, Marber MS, Parker PJ. The regulated assembly of a PKCepsilon complex controls the completion of cytokinesis. Nat Cell Biol. 2008; 10(8):891–901. [PubMed: 18604201]

27. Saurin AT, Brownlow N, Parker PJ. Protein kinase C epsilon in cell division: control of abscission. Cell Cycle. 2009; 8(4):549–55. [PubMed: 19197162]
28. Brownlow N, Pike T, Zicha D, Collinson L, Parker PJ. Mitotic catenation is monitored and resolved by a PKCε-regulated pathway. Nat Commun. 2014; 5:5685.doi: 10.1038/ncomms6685 [PubMed: 25483024]
29. Pike T, Brownlow N, Kjaer S, Carlton J, Parker PJ. PKCε switches Aurora B specificity to exit the abscission checkpoint. Nat Commun. 2016; 7:13853.doi: 10.1038/ncomms13853 [PubMed: 28004745]
30. Hämälistö S, Pouwels J, de Franceschi N, Saari M, Ivarsson Y, Zimmermann P, Brech A, et al. A ZO-1/α5β1-integrin complex regulates cytokinesis downstream of PKCε in NCI-H460 cells plated on fibronectin. PLoS One. 2013; 8(8):e70696. [PubMed: 23967087]
31. Takahashi M, Mukai H, Oishi K, Isagawa T, Ono Y. Association of immature hypophosphorylated protein kinase Cepsilon with an anchoring protein CG-NAP. J Biol Chem. 2000; 275(44):34592–6. [PubMed: 10945988]
32. Marchesi C, Dall'Asta V, Rotoli BM, Bianchi MG, Maggini C, Gazzola GC, Bussolati O. Chlorpromazine, clozapine and olanzapine inhibit anionic amino acid transport in cultured human fibroblasts. Amino Acids. 2006; (2):93–9. [PubMed: 16699818]
33. Klockenbusch C, Kast J. Optimization of formaldehyde cross-linking for protein interaction analysis of non-tagged integrin beta1. J Biomed Biotechnol. 2010; 2010:927585.doi: 10.1155/2010/927585 [PubMed: 20634879]
34. Chen D, Purohit A, Halilovic E, Doxsey SJ, Newton AC. Centrosomal anchoring of protein kinase C betaII by pericentrin controls microtubule organization, spindle function, and cytokinesis. J Biol Chem. 2004; 279(6):4829–39. [PubMed: 14594954]
35. Ma W, Koch JA, Viveiros MM. Protein kinase C delta (PKCdelta) interacts with microtubule organizing center (MTOC)-associated proteins and participates in meiotic spindle organization. Dev Biol. 2008; 320(2):414–25. [PubMed: 18602096]
36. Quann EJ, Liu X, Altan-Bonnet G, Huse M. A cascade of protein kinase C isozymes promotes cytoskeletal polarization in T cells. Nat Immunol. 2011; 12(7):647–54. [PubMed: 21602810]
37. Atwood SX, Li M, Lee A, Tang JY, Oro AE. GLI activation by atypical protein kinase C ι/λ regulates the growth of basal cell carcinomas. Nature. 2013 Feb 28; 494(7438):484–8. [PubMed: 23446420]
38. Yamada M, Toba S, Yoshida Y, Haratani K, Mori D, Yano Y, et al. LIS1 and NDEL1 coordinate the plus-end-directed transport of cytoplasmic dynein. EMBO J. 2008; 27(19):2471–83. [PubMed: 18784752]
39. Roossien DH, Miller KE, Gallo G. Ciliobrevins as tools for studying dynein motor function. Front Cell Neurosci. 2015; 9:252.doi: 10.1371/journal.pone.0080136 [PubMed: 26217180]
40. Yang Z, Tulu US, Wadsworth P, Rieder CL. Kinetochore dynein is required for chromosome motion and congression independent of the spindle checkpoint. Curr Biol. 2007; 17(11):973–80. [PubMed: 17509882]
41. Pfarr CM, Coue M, Grissom PM, Hays TS, Porter ME, McIntosh JR. Cytoplasmic dynein is localized to kinetochores during mitosis. Nature. 1990; 345(6272):263–5. [PubMed: 2139717]
42. Schroer TA. Dynactin. Annu Rev Cell Dev Biol. 2004; 20:759–79. [PubMed: 15473859]
43. Musacchio A, Salmon ED. The spindle-assembly checkpoint in space and time. Nat Rev Mol Cell Biol. 2007; 8(5):379–93. [PubMed: 17426725]
44. Howell BJ, McEwen BF, Canman JC, Hoffman DB, Farrar EM, Rieder CL, et al. Cytoplasmic dynein/dynactin drives kinetochore protein transport to the spindle poles and has a role in mitotic spindle checkpoint inactivation. J Cell Biol. 2001; 155(7):1159–72. [PubMed: 11756470]
45. Varma D, Monzo P, Stehman SA, Vallee RB. Direct role of dynein motor in stable kinetochore-microtubule attachment, orientation, and alignment. J Cell Biol. 2008; 182(6):1045–54. [PubMed: 18809721]
46. Damelin M, Bestor TH. The decatenation checkpoint. Br J Cancer. 2007; 96(2):201–5. [PubMed: 17211475]
47. Knight ZA, Shokat KM. Chemical genetics: where genetics and pharmacology meet. Cell. 2007; 128(3):425–430. [PubMed: 17289560]

48. Zhong A, Tan FQ, Yang WX. Chromokinesin: Kinesin superfamily regulating cell division through chromosome and spindle. Gene. 2016; 589(1):43–8. [PubMed: 27196062]

49. Raaijmakers JA, Tanenbaum ME, Medema RH. Systematic dissection of dynein regulators in mitosis. J Cell Biol. 2013; 201(2):201–15. [PubMed: 23589491]

Europe PMC Funders Author Manuscripts

Europe PMC Funders Author Manuscripts

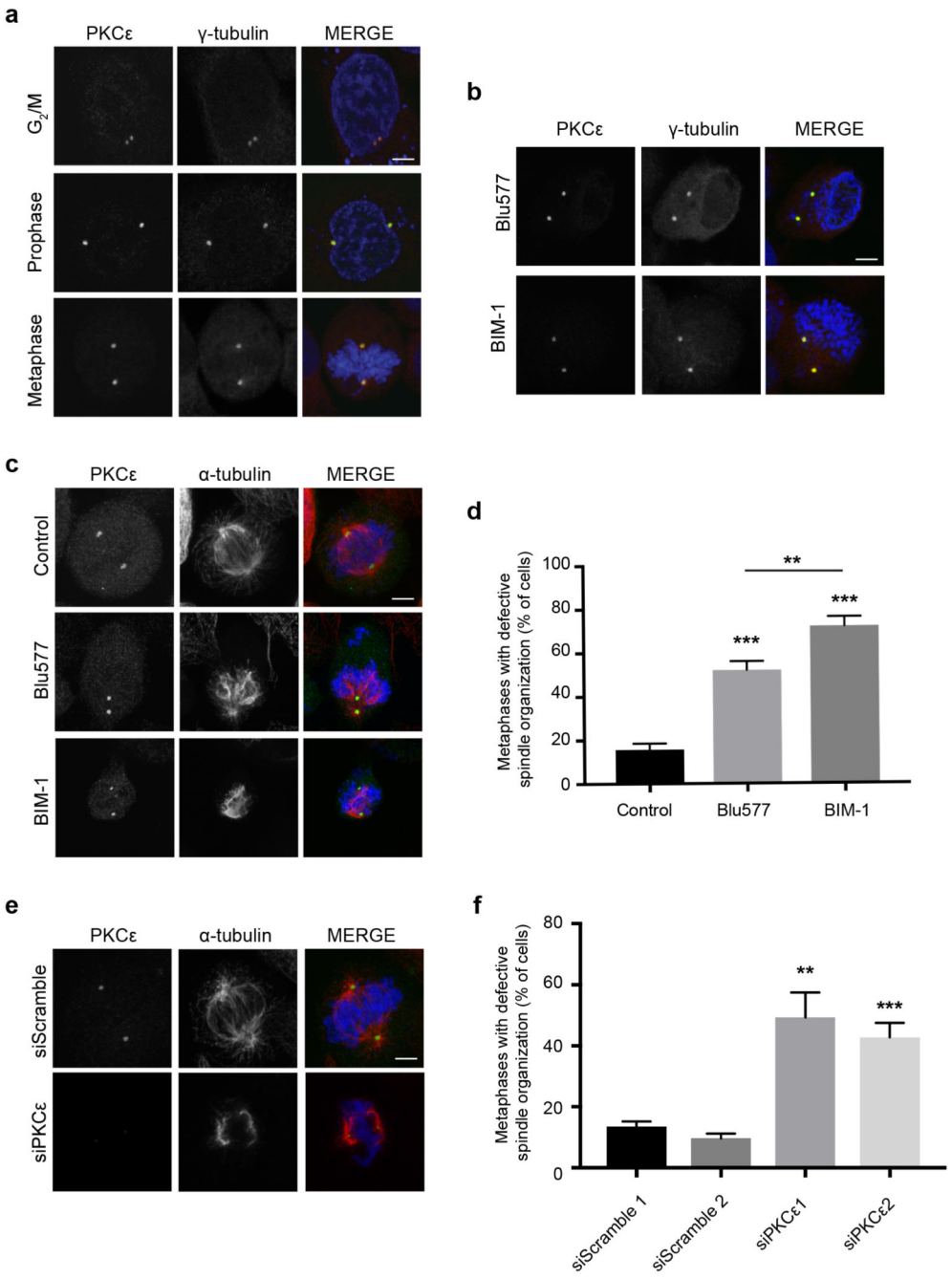

Figure 1.

(**a**)Localization of PKCε at the centrosomes in G2/M, prophase and metaphase. HeLa cells were stained with anti-PKCε (green), anti-γ-tubulin (red) and DAPI for DNA (blue). Scale bars,5 μm. (**b**)Blu577 or BIM-1 treatment do not affect PKCε localization at the centrosome. Cells were stained with anti-PKCε (green), anti-γ-tubulin (red) and DAPI (blue). Scale bars, 5 μm. (**c**)Representative images of HeLa cells treated with Blu577 and BIM-1. Cells were stained with anti-PKCε (green), anti-α-tubulin (red) and DAPI (blue). Scale bars, 5 μm. (**d**) The percentage of cells with a disrupted mitotic spindle is increased upon treatment with

PKCε inhibitors Blu577 and BIM-1. Quantification of cells in metaphase with a defective mitotic spindle. Chart shows mean of three experiments ± sd, n>100 per condition per experiment. ***P<0.001 *vs* CT. BIM-1 has stronger effect on mitotic spindle organization (**P<0.01 *vs* Blu577). (**e**) PKCε silencing using siRNA alters mitotic spindle organization in HeLa cells. Representative images and quantification (**f**) of HeLa cells treated for 48 hours with two different siRNA targeting PKCε; cells were stained with anti-PKCε (green), anti-γ-tubulin (red) and DAPI (blue). Scale bars, 5 μm. Chart shows mean of three experiments ± sd, n>100 per condition per experiment. **P<0.01 and ***P<0.001 *vs* SiScramble.

Europe PMC Funders Author Manuscripts

Europe PMC Funders Author Manuscripts

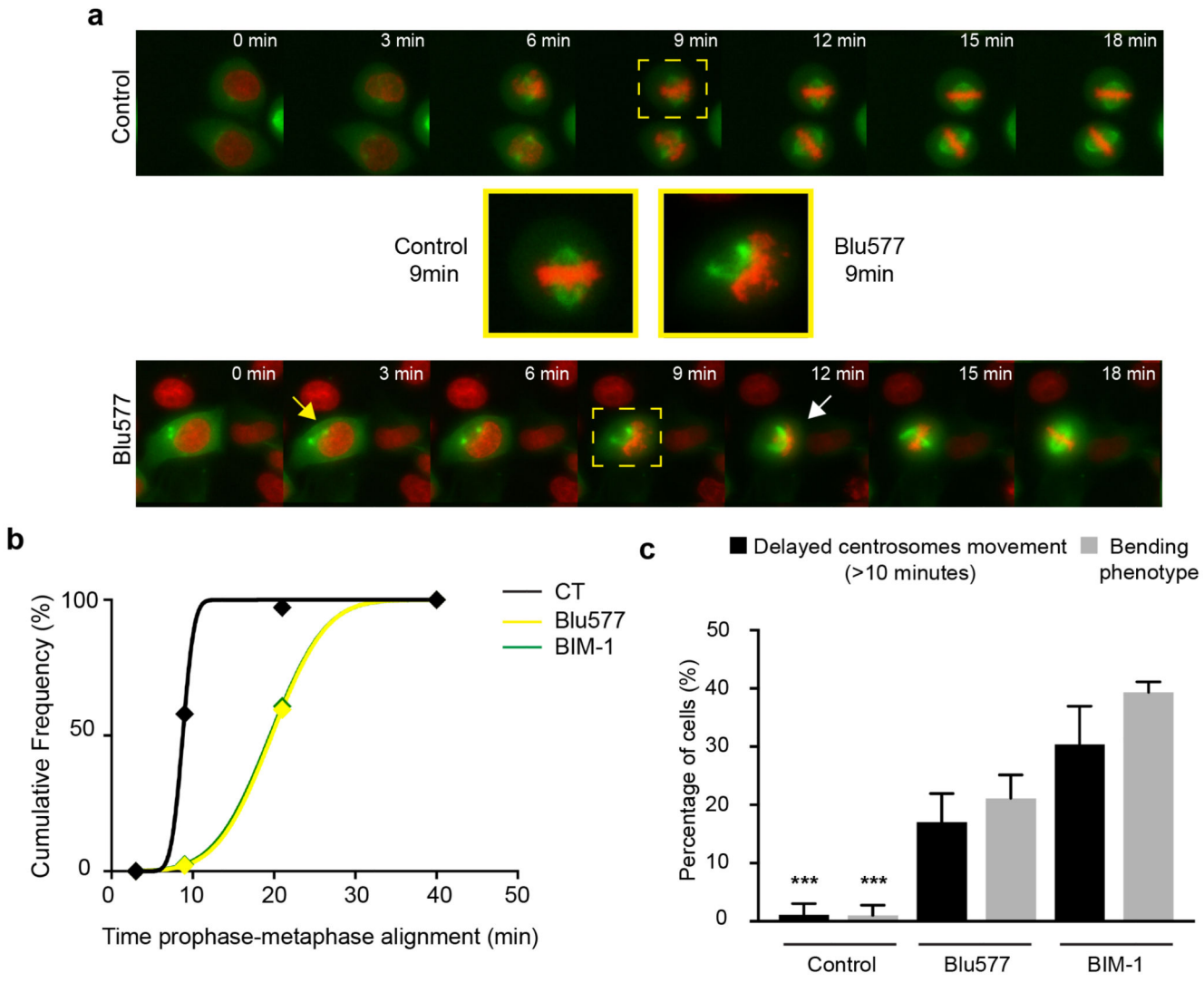

Figure 2.

(**a**) HeLa cells that stably express mCherry-H2B and GFP-Tubulin were imaged by time-lapse microscopy. Stills taken from time-lapse imaging of HeLa cells upon treatment with Blu577 and Control; time in minutes is marked in white. The yellow arrow indicates the centrosome delay. The white arrow indicates the "bending" phenotype. As shown in the yellow field, representative control cell is in metaphase at 9 minutes, whereas cells treated with Blu577 are still in prophase/prometaphase (**b**) Graph shows the cumulative frequency of cells that took 3-9 minutes (quick), 10-20 minutes (medium) and 21-39 minutes (slow) from prophase to metaphase alignment upon PKCε inhibition. Chart shows the average of three experiments ± sd, n>30 per condition per experiment. ***P<0.001 *vs* CT. (**c**) Graph represents the percentage of cells which centrosome took more than 10 minutes to reach the opposite poles (black charts) and the cells presenting the "bending" phenotype (grey). Charts show the average of three experiments ± sd, n>30 per condition per experiment. ***P<0.001 Blu577 and BIM-1 *vs* CT.

Europe PMC Funders Author Manuscripts

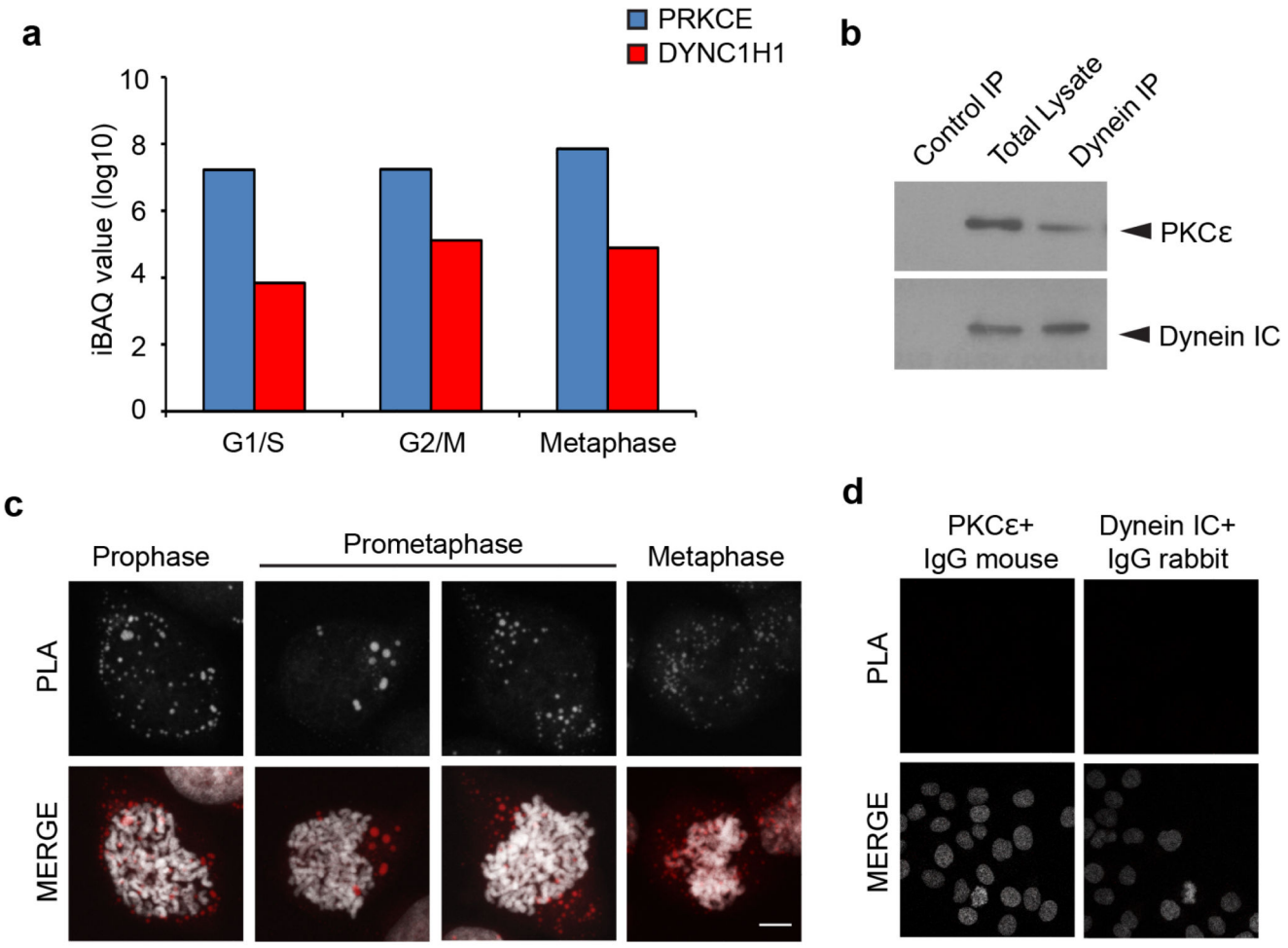

Figure 3.

(**a**) Bar graph comparing PRKCE (blue) and DYNC1H1 (red) at G1/S, G2/M and metaphase stages of the cell cycle using log10 transformed intensity based absolute quantification (iBAQ) values. An order of magnitude difference is observed for DYNC1H1 at G1 compared to G2 and metaphase in contrast to PRKCE. (**b**) Co-immunoprecipitation assay was performed using anti-Dynein IC antibody in HeLa cells synchronized in prometaphase/metaphase and cross-linked using 1% formaldehyde. IgG-Mouse used as control, Total lysate and Dynein IP were analysed by western blot and probed for PKCε and for Dynein IC to assess the efficiency of the assay. Under the extraction conditions used, there is a ~ 1:2 relative ratio of PKCε:Dynein IC in cells enriched in prometaphase/metaphase. (**c**) Detection of PKCε and Dynein IC interaction in HeLa cells using the *in situ* Proximity Ligation Assay (PLA). The images show a maximum intensity projection of the raw image; PLA signals are shown in red and DNA in grey. Scale bars, 5 μm. (**d**) Proximity Ligation Assay (PLA) negative control reaction using rabbit anti-PKCε antibody with anti-IgG mouse (left) and mouse anti-Dynein IC antibody with anti-IgG rabbit (right).

Europe PMC Funders Author Manuscripts

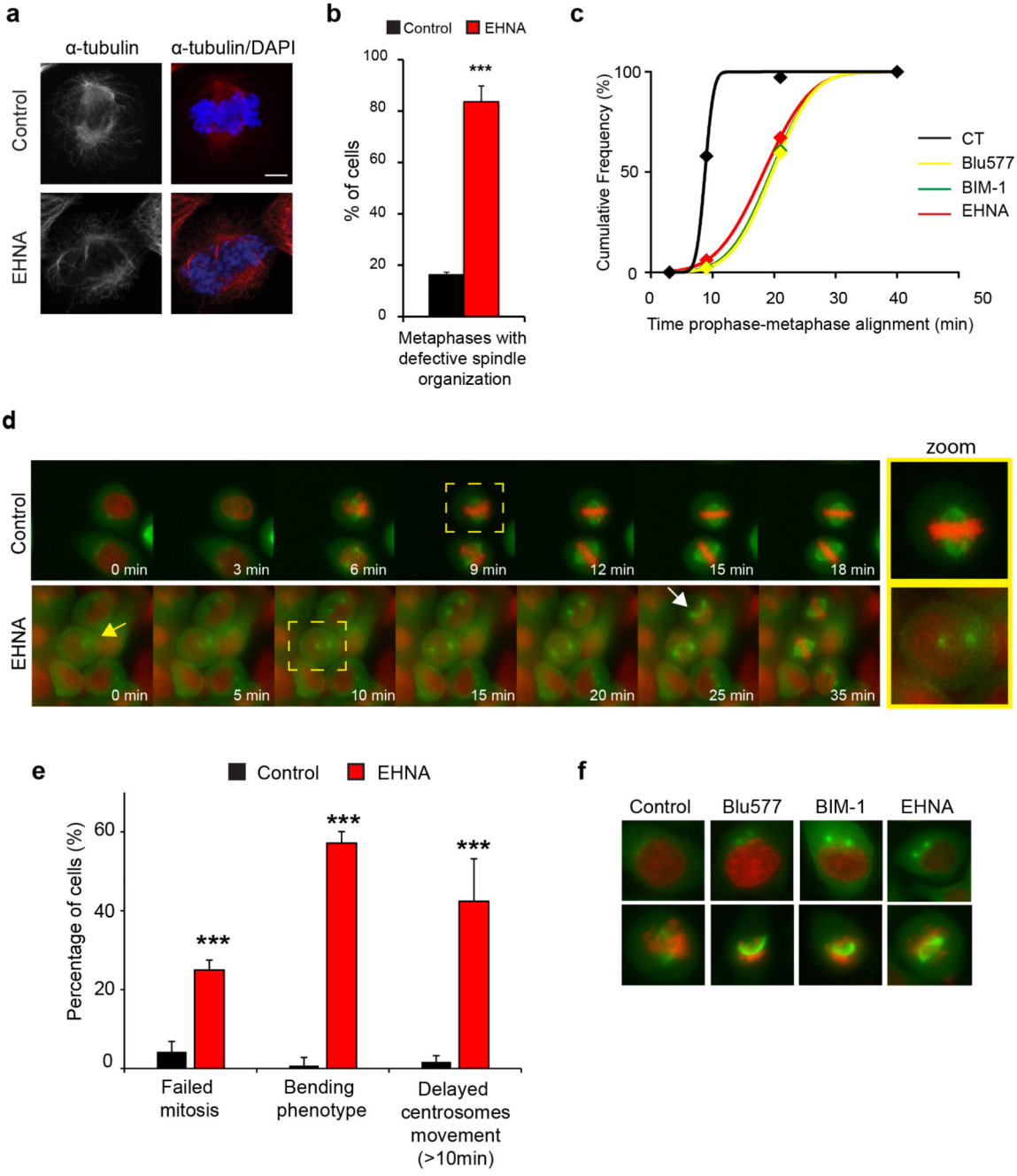

Figure 4.

(**a**)Confocal images of HeLa cells untreated or treated for 1 hour with EHNA. α-tubulin is represented in red and DNA in blue (DAPI). Scale bar, 5 μm. (**b**)The amount of mitotic HeLa cells treated with EHNA (red) with a disrupted spindle is significantly higher compared with control (black). Chart shows mean of three experiments ± sd, n>100 per condition per experiment. ***P<0.001 vs CT. (**c-f**) Mitotic events were live-imaged in HeLa cells stably expressing mCherry-H2B (red) and GFP-tubulin (green). (**c**) The graph shows the cumulative frequency of cells that took 3-9 minutes (quick), 10-20 minutes (medium)

and 21-39 minutes (slow) from prophase to metaphase alignment upon Blu577, BIM-1 and EHNA treatment. Chart shows the average of three experiments ± sd, n>30 per condition per experiment. ***P<0.001 vs CT. (**d**) Stills taken from time-lapse imaging of HeLa cells with or without EHNA treatment; as shown in the yellow box and in the zoom, representative control cell is in metaphase at 9 minutes, whereas the cell treated with EHNA is still in prophase. The time in minutes is marked in white. The yellow arrow indicates the centrosome delay, white arrow indicates the “bending” phenotype. (**e**)The graphs describes that EHNA treatment (red) causes an increase of the percentage of cells unable to complete mitosis, an increase of the number of cells with delayed centrosome movement (> 10 minutes) and with the “bending” phenotype. Charts show the average of three experiments ± sd, n>30 per condition per experiment. ***P<0.001 vs CT. (**f**)Representative images of the centrosome delay (upper lane) and the “bending” phenotype (lower lane) taken from live imaging of HeLa cells upon EHNA, Blu577 and BIM-1 treatments.

Europe PMC Funders Author Manuscripts

Europe PMC Funders Author Manuscripts

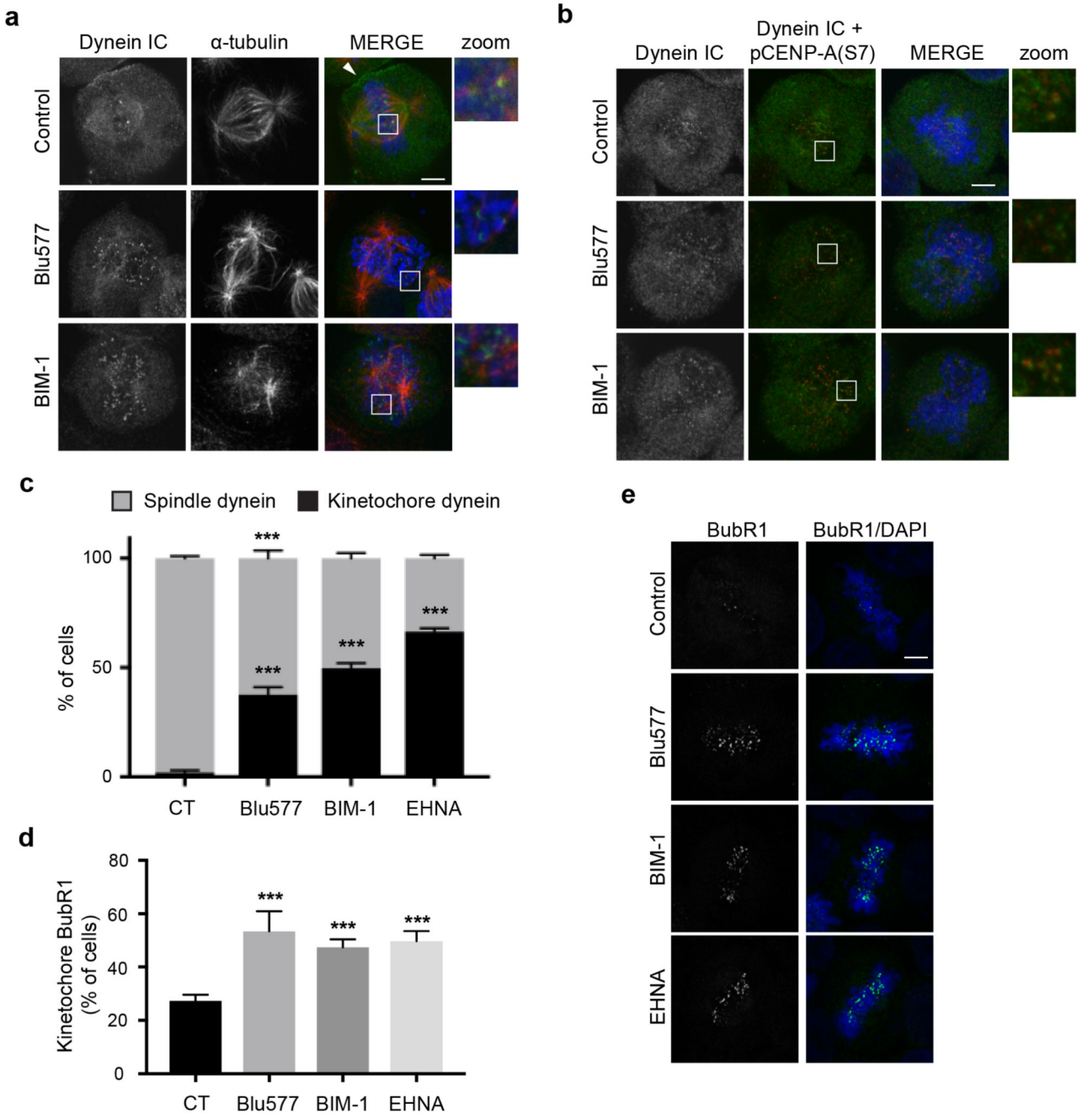

Figure 5.

(**a**)Confocal images of HeLa cells treated with Blu577 and BIM-1 for 1 hour, fixed and stained with anti-Dynein IC(green), α-tubulin(red) and DAPI(blue). In a control cell in metaphase (upper panel), Dynein IC is localized at the plus end of the microtubules (inset), at the cortex (arrow) and along the microtubules of the mitotic spindle. In HeLa cells treated with Blu577 and BIM-1, the mitotic spindle is disorganised, the chromatids are condensed prophase/prometaphase-like and Dynein is localized at the kinetochores (inset).

(**b**)Representative images of HeLa cells treated with Blu577 and BIM-1 for 1 hour, fixed and

stained with anti-Dynein IC (green), pCENP-A(S7) (red) and DAPI (blue). In the control, Dynein IC localizes with pCENP-A(S7) at the plus end of the microtubules (upper panel), whereas it is coupled with the kinetochores when PKCε is inhibited (Blu577, middle panel; BIM-1, lower panel). (**c**)Quantification of mitotic HeLa cells with Dynein IC labelled at the spindle (grey charts) and at the kinetochores (black charts). Chart shows mean of three experiments ± sd, n>100 per condition per experiment. ***P<0.001 *vs* CT. (**d**)Quantification of the amount of HeLa cells in metaphase with BubR1 retained at the kinetochores. Chart shows mean of three experiments ± sd, n>50 per condition per experiment. ***P<0.001 vs CT. (**e**)Representative images of BubR1 staining (green) and DNA (blue) in metaphase cells upon the different treatments. Scale bars, 5 μm.

Europe PMC Funders Author Manuscripts

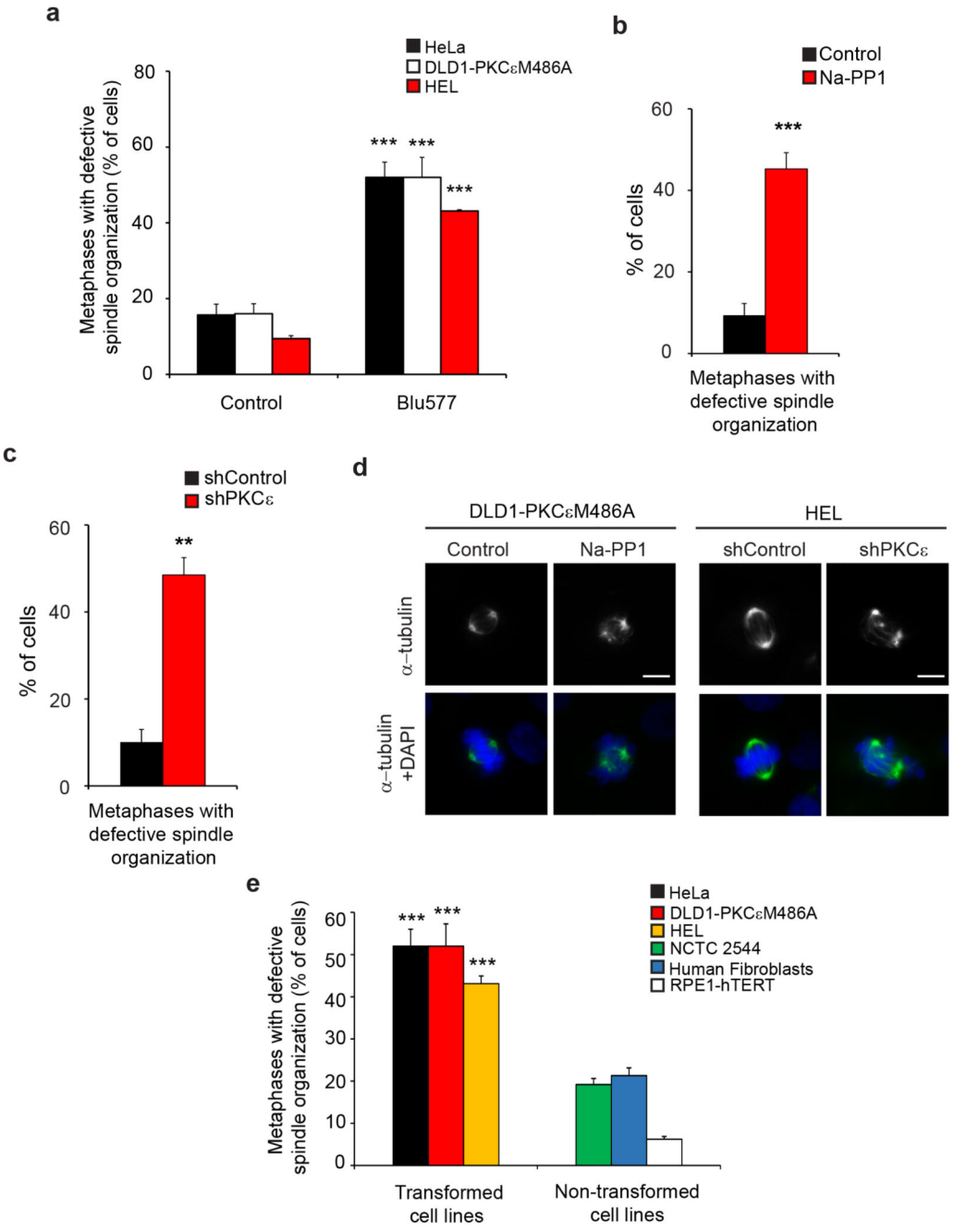

Figure 6.

(**a**) PKCε inhibition using Blu577 results in defects in mitotic spindle organization in HeLa (black), DLD1-PKCεM486A (white) and HEL (red) cells. ***P<0.001 vs Control. (**b**)Quantification of DLD1 cells in metaphase with defective mitotic spindle, with (red) or without (black) Na-PP1 to inhibit PKCε. ***P<0.001 vs Control. (**c**)Quantification of HEL cells in metaphase with defective mitotic spindle, treated with shControl (black) or shPKCε (red). **P<0.01 vs shControl. (**d**)Representative images of DLD1 (left) and HEL cells (right), treated with or without the respective PKCε inhibitor. Cells were stained using anti-

α-tubulin antibody (green) and DAPI (blue). Scale bar, 10μm. (**e**) Quantification of defective mitotic spindle in transformed cell lines HeLa (black), DLD1 (red) and HEL (yellow) compared with non-transformed cell lines NCTC 2544 (green), Human Fibroblast (blue) and RPE1-hTERT (white). All cell lines were treated with the PKCε inhibitor Blu577 for 1 hour. ***P<0.001. Charts in all panels show the mean of three experiments ± sd, n>100 per condition per experiment using HeLa and DLD1-PKCεM486A, NCTC 2544, Human Fibroblast and RPE1-hTERT cells, n=30 per condition per experiment using HEL cells.